

Modelling and numerical simulations of a pendulum elastically suspended and driven by frictional contact with rotating disk (BIF204-15)

Grzegorz Kudra, Jan Awrejcewicz

Abstract: The work concerns modelling and numerical simulations of a special kind of physical pendulum frictionally driven. The pendulum's joint is suspended elastically in the plane of the motion resulting in the full plane motion of the pendulum and in three degrees of freedom of the analysed mechanical system. The pendulum is driven by frictional contact with a disk with a constant angular velocity. Examples of self-excited oscillations and bifurcation dynamics of the pendulum are presented. Majority of the work focuses on efficient approximate modelling of the resultant friction force and moment occurring on the contact surface.

1. Introduction

There are plenty of examples of mechanical systems, where friction plays a crucial role in their dynamical properties and behavior. Friction can be a desirable phenomenon or not, but in both cases its appropriate and efficient mathematical modelling is an important part of analysis and synthesis of mechanical systems with frictional contacts. The classically understood friction model is a relation between single component of friction force and one-dimensional relative displacement of the contacting bodies. This relation can possess different levels of complexity, beginning with the classical Coulomb friction law and ending with advanced relations, where often additional state variables are defined. These kinds of models can be applied directly during mathematical description and analysis of dynamical systems with frictional contacts, where at each element of the contact the same relative motion of the contacting surfaces occurs. But in real life one can encounter many examples of mechanical systems, where the above assumption cannot lead to correct results. One can give such examples like dynamics of rolling bearings, billiard balls, different kinds of tops, the wobblestone, polishing machine, disk clutches and many others. Exact and correct results can be always obtained by detailed physical modelling and space discretization in vicinity of the contact. But this approach leads to computation cost increase and is not appropriate in fast numerical simulations. This is the reason of the interest of many researchers in looking for simple approximate models of contact forces, which would be suitable for fast and realistic simulations of the certain classes of mechanical systems with frictional contacts.

Contensou [1] noticed that if the product of the normal component of the relative angular velocity of the contacting bodies and size of the contact is sufficiently large then one should take into account the coupling between the friction force and moment. He proposed an integral model of the resultant friction forces under assumption of fully developed sliding and Coulomb friction law valid on each element of the circular contact. The results of Contensou were then significantly developed by Zhuravlev [2], who presented exact analytical solution to the Contensou's integral model and also proposed the corresponding approximant models based on the Padé expansions. Further developments and generalizations of the approximant models of the contact forces, including rolling resistance, assuming elliptical contact area, are proposed in the work [3]. Special regularizations of these models can be found in [4, 5], which allow to avoid singularities for vanishing relative motion as well as take into account the different values of the static and kinetic friction coefficients.

Stamm and Fidin [6] proposed a regularized two-dimensional model of friction forces appearing on finite plane area based on elasto-visco-plastic theory, but requiring discretization of the contact area. They applied their model in modelling and analysis of a disk-on-a-disk system being to certain extent a counterpart of a disk clutch, where alternating sliding and sticking solutions can occur [7]. In the work [8] there are presented results of analytical studies of the similar system, where the approximations based on Taylor's expansion of the friction force and moment for fully developed sliding are used.

In the present work the authors apply their earlier developed models of the resultant friction force and moment in modelling and numerical simulations of the mechanical system being a certain modification of the disk-on-a-disk system analyzed in the works [7, 8].

2. Modelling of friction forces

Let us consider a circular contact area of dimensionless form exhibited in figure 1, where one assumed: i) the fully developed sliding; ii) Classical Coulomb friction law valid on each element of the contact; iii) constant friction coefficient; iv) that the relative motion of the contacting surfaces is a plane motion of rigid bodies. There are also assumed the following relations between real and non-dimensional quantities describing the contact: $\hat{\mathbf{T}}_s = \mu \hat{N} \mathbf{T}_s$, $\hat{\mathbf{M}}_s = \mu \hat{N} \hat{a} \mathbf{M}_s$, $\hat{\sigma}(x, y) = (\hat{N} / \hat{a}^2) \sigma(x, y)$, $\hat{\mathbf{v}}_s = \hat{a} \mathbf{v}_s$ and $\hat{\boldsymbol{\omega}}_s = \boldsymbol{\omega}_s$, where $\hat{\mathbf{T}}_s$ and $\hat{\mathbf{M}}_s$ are the real resultant friction force and moment loading the contact and reduced to the center A of the contact F , \mathbf{T}_s and \mathbf{M}_s – the corresponding non-dimensional resultant friction force and moment, μ – friction coefficient, \hat{N} – real normal loading of the contact, \hat{a} – characteristic dimension of the contact (in this case real radius of the contact F), $\hat{\sigma}$ and σ – real and dimensionless contact pressure, $\hat{\mathbf{v}}_s$ and \mathbf{v}_s – relative real and dimensionless relative linear velocity at the point A , $\hat{\boldsymbol{\omega}}_s = \boldsymbol{\omega}_s$ – relative angular velocity in the plane of the contact. Note that time in all the introduced quantities is real.

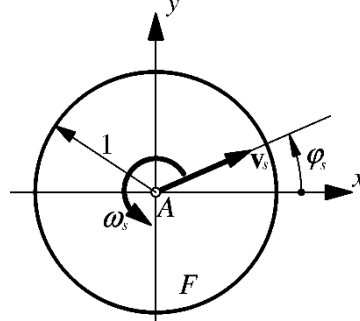


Figure 1. The contact area.

Assuming that $\mathbf{T}_s = -T_{sx}\mathbf{e}_x - T_{sy}\mathbf{e}_y$, $\mathbf{M}_s = -M_s\mathbf{e}_z$, $\mathbf{v}_s = v_{sx}\mathbf{e}_x + v_{sy}\mathbf{e}_y$ and $\boldsymbol{\omega}_s = \omega_s\mathbf{e}_z$, where \mathbf{e}_ξ is the unit vector along the axis ξ , one can find the following integral expressions:

$$\begin{aligned} T_{sx} &= \iint_{dF} n(x, y) (v_{sx} - \omega_s y) dx dy, \\ T_{sy} &= \iint_{dF} n(x, y) (v_{sy} + \omega_s x) dx dy, \\ M_s &= \iint_{dF} n(x, y) (\omega_s(x^2 + y^2) + v_{sy}x - v_{sx}y) dx dy, \end{aligned} \quad (1)$$

where

$$n(x, y) = \sigma(x, y) \left((v_{sx} - \omega_s y)^2 + (v_{sy} + \omega_s x)^2 \right)^{-1/2}.$$

Since the model (1) requires integration over the contact area at each time step, it is not suitable tool for fast and reliable numerical simulations. Based on the results presented in the previous works of the authors [3] and assuming the constant dimensionless contact pressure distribution on circular contact area $\sigma(x, y) = 1/\pi$, one can derive the following two sets of approximations of the integral model (1)

$$\begin{aligned} T_{sx}^{(I_{0,0})} &= \frac{v_{sx}}{\left((v_{sx}^2 + v_{sy}^2)^{\frac{m}{2}} + b^m |\omega_s|^m \right)^{\frac{1}{m}}}, \\ T_{sy}^{(I_{0,0})} &= \frac{v_{sy}}{\left((v_{sx}^2 + v_{sy}^2)^{\frac{m}{2}} + b^m |\omega_s|^m \right)^{\frac{1}{m}}}, \\ M_s^{(I_{0,0})} &= \frac{\frac{2}{3} b \omega_s}{\left((v_{sx}^2 + v_{sy}^2)^{\frac{m}{2}} + b^m |\omega_s|^m \right)^{\frac{1}{m}}}. \end{aligned} \quad (2)$$

and

$$\begin{aligned}
T_{sx}^{(l_{1,1})} &= \frac{(v_{sx}^2 + v_{sy}^2 + b\omega_s^2)v_{sx}}{\left((v_{sx}^2 + v_{sy}^2)^{\frac{3m}{2}} + b^m|\omega_s|^{3m}\right)^{\frac{1}{m}}}, \\
T_{sy}^{(l_{1,1})} &= \frac{(v_{sx}^2 + v_{sy}^2 + b\omega_s^2)v_{sy}}{\left((v_{sx}^2 + v_{sy}^2)^{\frac{3m}{2}} + b^m|\omega_s|^{3m}\right)^{\frac{1}{m}}}, \\
M_s^{(l_{1,1})} &= \frac{\frac{2}{3}b\omega_s^3 + \frac{1}{4}\omega_s(v_{sx}^2 + v_{sy}^2)}{\left((v_{sx}^2 + v_{sy}^2)^{\frac{3m}{2}} + b^m|\omega_s|^{3m}\right)^{\frac{1}{m}}}.
\end{aligned} \tag{3}$$

The approximations (2-3), after the replacements $v_{sx} = v_s \cos \varphi_s$ and $v_{sy} = v_s \sin \varphi_s$, fulfil the following properties of the integral model (1)

$$\begin{aligned}
\left. \frac{\partial^i f^{(l_{n1}, n2)}}{\partial v_s^i} \right|_{v_s=0} &= \left. \frac{\partial^i f}{\partial v_s^i} \right|_{v_s=0}, \quad i = 1, \dots, n_1, \\
\left. \frac{\partial^j f^{(l_{n1}, n2)}}{\partial \omega_s^j} \right|_{\omega_s=0} &= \left. \frac{\partial^j f}{\partial \omega_s^j} \right|_{\omega_s=0}, \quad j = 1, \dots, n_2,
\end{aligned} \tag{4}$$

where $f = T_{sx}, T_{sy}, M_s$, while m and b are arbitrary constants. Note that the above approximations possess the same denominators, which is not necessary in general (see [3]), but allows for application of the later presented special form of regularization.

In order to make easier the comparison of the functions (1-3), one introduces the spherical coordinates

$$v_{sx} = \lambda_s \cos \theta_s \cos \varphi_s, \quad v_{sy} = \lambda_s \cos \theta_s \sin \varphi_s, \quad \omega_s = \lambda_s \sin \theta_s. \tag{5}$$

The parameters m and b are optimized by searching for the best fitting of the corresponding functions on the representative (in the case of circularly symmetric contact pressure distribution) field $\theta_s \in [0, \pi/2]$ and $\varphi_s = 0$. For the functions (2) one found $b = 1.744$ and $m = 0.674$, while for the approximations (3) one obtained $b = 0.765$ and $m = 0.452$. The corresponding plots are exhibited in figure 2. In the further modelling process the approximations (3) will be used.

In the works [4, 5] a special kind of regularization of the models of the type (2-3) was proposed, allowing to avoid singularity for vanishing relative motion of the contacting surfaces, but also to model the situation where the static friction coefficient is greater than the kinetic one. Applying that approach to the components (3) one gets

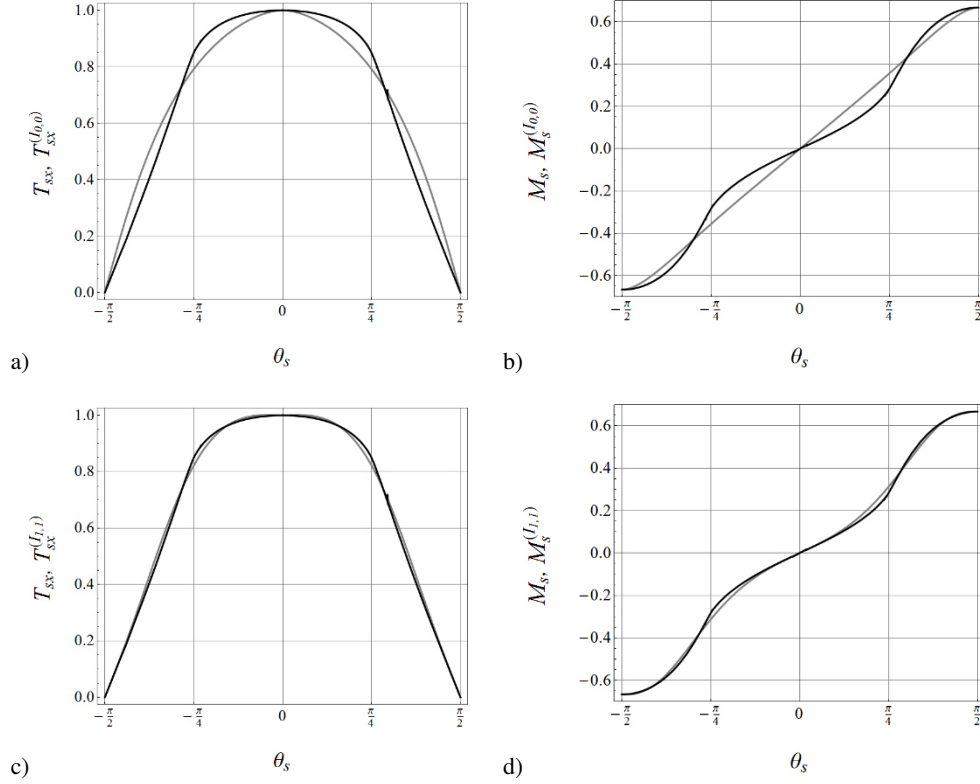


Figure 2. Comparison of the approximate components $T_{sx}^{(l_{0,0})}$ (a), $M_s^{(l_{0,0})}$ (b), $T_{sx}^{(l_{1,1})}$ (c), $M_s^{(l_{1,1})}$ (d) of the friction model (grey lines) with the corresponding full integral components T_{sx} and M_s (black lines), for $\varphi_s = 0$.

$$\begin{aligned}
 T_{sx\varepsilon}^{(l_{1,1})} &= (v_{sx}^2 + v_{sy}^2 + b\omega_s^2)v_{sx}\lambda_{sb\varepsilon}, \\
 T_{sy\varepsilon}^{(l_{1,1})} &= (v_{sx}^2 + v_{sy}^2 + b\omega_s^2)v_{sy}\lambda_{sb\varepsilon}, \\
 M_{s\varepsilon}^{(l_{1,1})} &= \left(\frac{2}{3}b\omega_s^3 + \frac{1}{4}\omega_s(v_{sx}^2 + v_{sy}^2)\right)\lambda_{sb\varepsilon},
 \end{aligned} \tag{6}$$

where

$$\lambda_{sb\varepsilon} = \frac{1}{\sqrt{\left(\left(v_{sx}^2 + v_{sy}^2\right)^{\frac{3m}{2}} + b^m|\omega_s|^{3m}\right)^{\frac{2}{m}} + \varepsilon^6}} + \eta'(\eta) \frac{\varepsilon^9}{\left(\left(v_{sx}^2 + v_{sy}^2\right)^{\frac{3m}{2}} + b^m|\omega_s|^{3m}\right)^{\frac{2}{m}} + \varepsilon^6},$$

and where ε is a small numerical parameter. The coefficient η' is a function of the parameter η equal to the maximum magnitude of the resultant dimensionless friction force (or $\eta = \mu_0/\mu$, where μ_0 is the

static friction coefficient). This function can be approximated as $\eta'(\eta) \approx -13.607 + 30.893\eta - 22.01\eta^2 + 5.878\eta^3$ for $\eta \in [1, 1.3]$ and $\eta'(\eta) \approx -2.41 + 3.985\eta - 0.3581\eta^2 + 0.0493\eta^3$ for $\eta \in [1.3, 2.7]$, with the error $|\Delta\eta| < 0.001$ (see [5]). Figure 3 exhibits exemplary plots of the model (6) near zero relative motion, for $\theta_s = \pi/4$, $\varphi_s = 0$, $\eta = 2$ and $\varepsilon = 10^{-3}$.

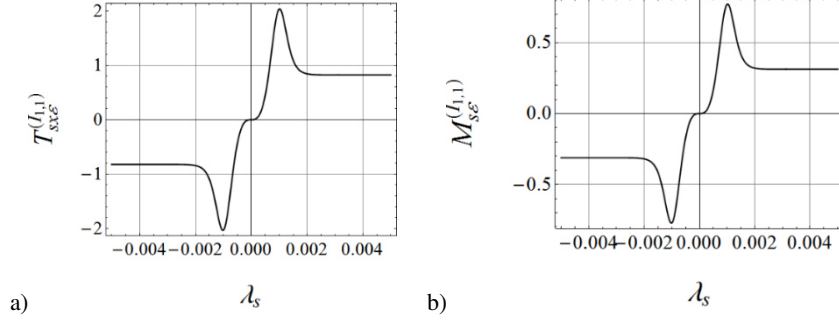


Figure 3. Approximations $T_{sx\varepsilon}^{(I_{1,1})}$ (a), $M_{s\varepsilon}^{(I_{1,1})}$ (b) near zero relative motion - for $\theta_s = \pi/4$, $\varphi_s = 0$, $\eta'(2) = 4.479$ and $\varepsilon = 10^{-3}$.

3. Mathematical model of the pendulum

In figure 4 there is presented a physical conception of the special mechanical system, being a certain modification of the disk-on-a-disk system analyzed in the works [7, 8]. A physical pendulum of mass M and moment of inertia B with respect to the mass center C is rotationally connected, by the use of the joint A , a light platform. The platform is mounted on the support by the use of elasto-damping elements in such a way, that it cannot rotate. The origin O of the introduced coordinate system OXY is defined as a position of the point A of the pendulum in its equilibrium position in the case of no friction forces acting on the mechanical system. The pendulum is equipped with a flat disk of radius R centered in the point A . This disk is in contact with a larger rotating rigid body performing pure rotational motion with constant angular velocity ω_0 about the center S . It assumed a constant contact pressure distribution and Coulomb friction law on each element of the circular contact between the bodies.

The governing equations of the presented mechanical system read

$$\begin{aligned}
 M(\ddot{X}_A - e\ddot{\varphi} \sin \varphi - e\dot{\varphi}^2 \cos \varphi) + k_X X_A + c_X \dot{X}_A + \mu \widehat{N} T_{sx\varepsilon}^{(I_{1,1})} &= 0, \\
 M(\ddot{Y}_A + e\ddot{\varphi} \cos \varphi - e\dot{\varphi}^2 \sin \varphi) + k_Y Y_A + c_Y \dot{Y}_A + \mu \widehat{N} T_{sy\varepsilon}^{(I_{1,1})} &= 0, \\
 B\ddot{\varphi} + e(Mg + k_X X_A + c_X \dot{X}_A + \mu \widehat{N} T_{sx\varepsilon}^{(I_{1,1})}) \sin \varphi + \\
 -e(k_Y Y_A + c_Y \dot{Y}_A + \mu \widehat{N} T_{sy\varepsilon}^{(I_{1,1})}) \cos \varphi + c_\varphi \dot{\varphi} + \mu \widehat{N} R M_{s\varepsilon}^{(I_{1,1})} &= 0,
 \end{aligned} \tag{7}$$

where X_A and Y_A are the coordinates of the point A; φ – angular position of the pendulum; $e = AC$ – position of the mass center C; k_X and k_Y – stiffness coefficients of the elements supporting the rotational joint A; c_X and c_Y – the corresponding damping coefficients; c_φ – the coefficient of damping in the rotational joint A; μ – kinetic friction coefficient; \hat{N} – normal loading of the contact; X_S and Y_S – the coordinates of the point S; g – gravitational acceleration. As a model of the resultant friction force and moment the relations (6) are applied.

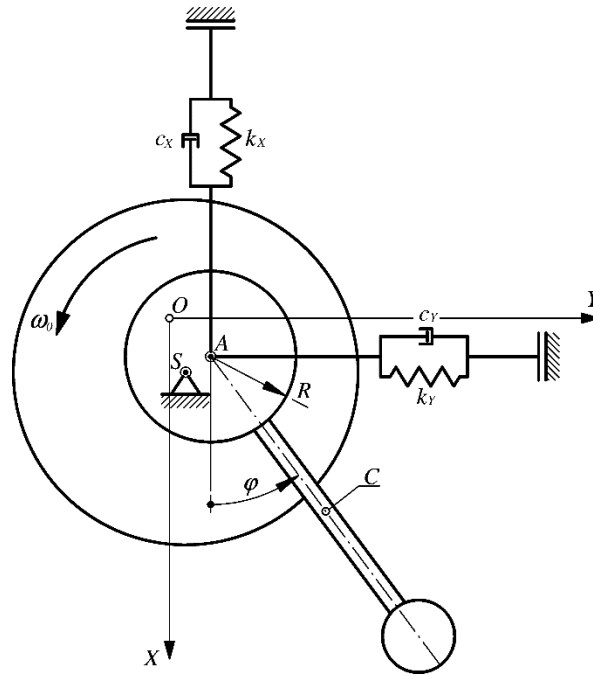


Figure 4. The physical concept of the mechanical system.

The kinematic arguments of the functions (6) read

$$\begin{aligned} \omega_s &= \dot{\varphi} - \omega_0, \\ v_{sx} &= \frac{\dot{X}_A + \omega_0(Y_A - Y_S)}{R}, \\ v_{sy} &= \frac{\dot{Y}_A - \omega_0(X_A - X_S)}{R}. \end{aligned} \quad (8)$$

4. Numerical simulations

In all the presented in this section numerical simulations the following parameters are fixed: $g = 9.81 \text{ m/s}^2$, $b = 0.452$, $m = 0.765$ and $\varepsilon = 10^{-3}$.

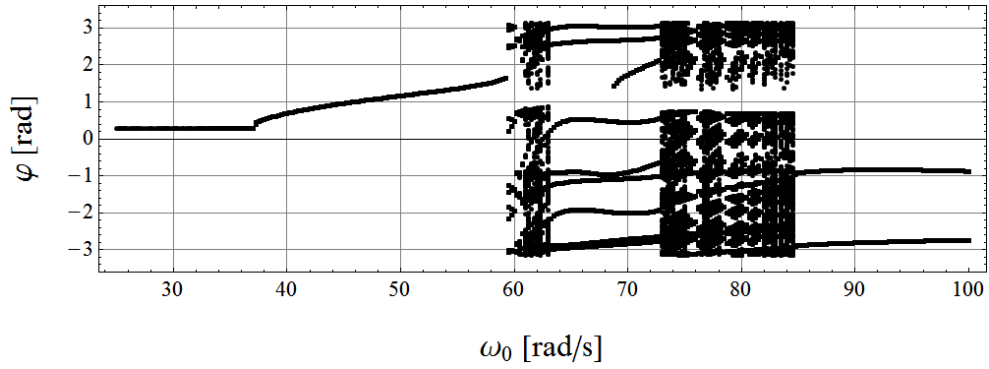


Figure 5. Bifurcation diagram with angular frequency ω_0 as a control parameter.

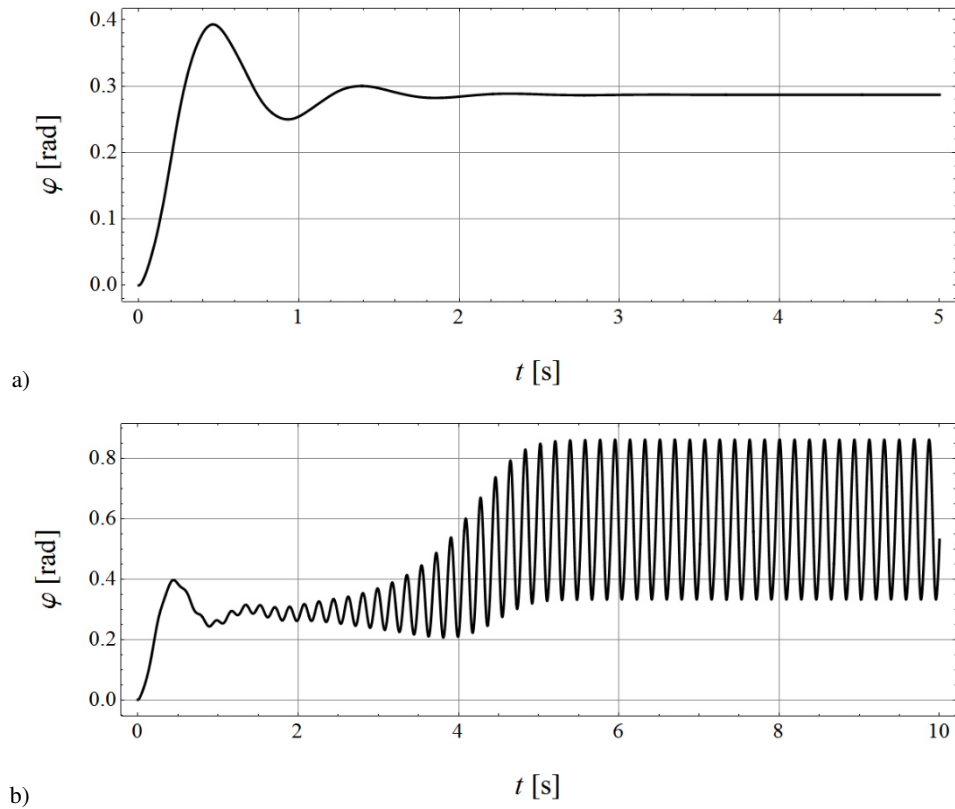


Figure 6. Examples of the system's behavior corresponding to the bifurcation diagram presented in figure 5, for $\omega_0 = 30$ rad/s (a), $\omega_0 = 40$ rad/s (b).

In figure 5 there is presented a bifurcation diagram of the system exhibited in figure 4 with the angular velocity ω_0 playing a role of a bifurcational parameter. The remaining system parameters read: $M = 1.2$ kg, $B = 0.01$ kg m², $e = 0.1$ m, $k_X = k_Y = 1000$ N/m, $c_X = c_Y = 0.1$ N s/m, $c_\varphi = 0.1$ N m s, $X_s = 0$ m, $Y_s = 0$ m, $R = 0.02$ m, $\hat{N} = 25$ N, $\mu = 1$ and $\eta = 1$ (the static friction coefficient is equal to the kinetic one). For low angular velocities one observe a stable equilibrium position – see figure 6(a), where for $\omega_0 = 30$ rad/s the corresponding time history of the angle φ is presented. For the greater values of ω_0 a stable periodic attractor appears - see figure 6(b). Further increase of ω_0 leads to rich bifurcational and irregular dynamics, with full rotations of the pendulum – see figure 7.

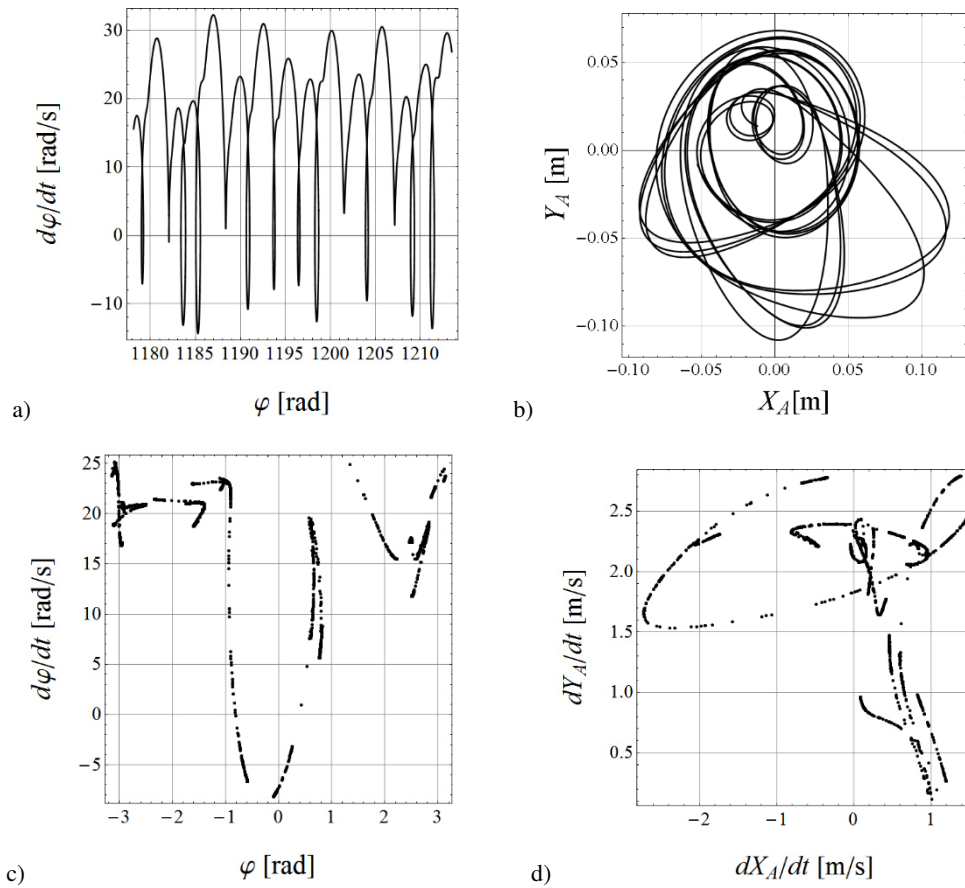


Figure 7. Trajectory of the system (a-b) and Poincaré section (c-d) corresponding to the bifurcation diagram presented in figure 5 for $\omega_0 = 61.5$ rad/s.

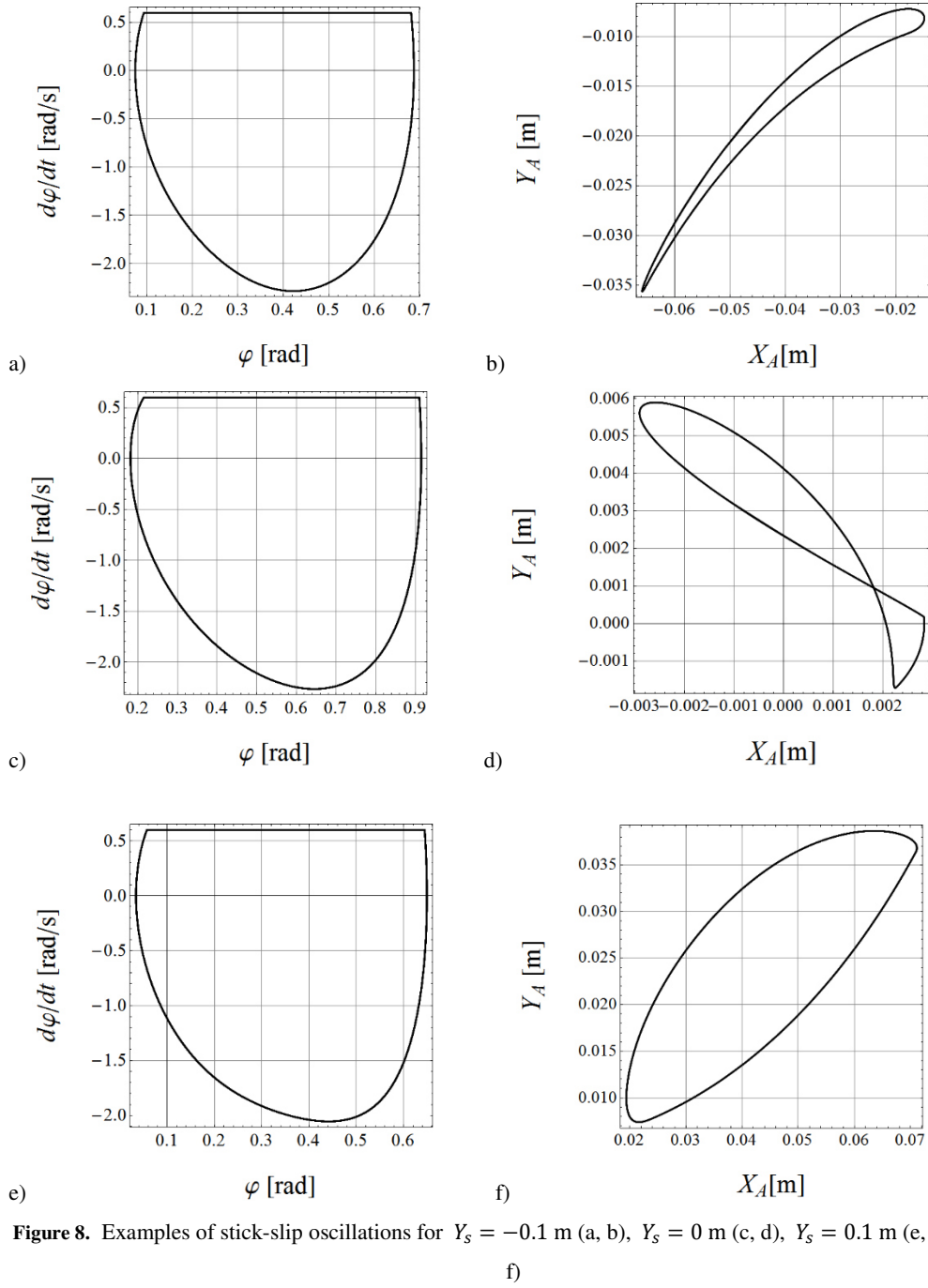


Figure 8. Examples of stick-slip oscillations for $Y_s = -0.1$ m (a, b), $Y_s = 0$ m (c, d), $Y_s = 0.1$ m (e, f)

In figure 8 there are presented examples of periodic stick-slip oscillations of the investigated mechanical system, where the following parameters are assumed: $M = 1.2$ kg, $B = 0.01$ kg m², $e = 0.1$ m, $k_X = k_Y = 100$ N/m, $c_X = c_Y = 0.1$ N s/m, $c_\varphi = 0.1$ N m s, $X_S = 0$ m, $\omega_0 = 0.6$ rad/s, $R = 0.1$ m, $N = 6$ N, $\mu = 1$ and $\eta = 2.5$. The position of the joint S along the axis X is different for each of the presented solutions: $Y_S = -0.1$ m (a, b), $Y_S = 0$ m (c, d), $Y_S = 0.1$ m (e, f).

5. Conclusions

In the work there have been presented examples of models of the resultant friction force and moment based on the previous works of the authors. They are simple functions, which can be an effective substitute for the exact integral model, suitable for fast and realistic computer simulations of a certain class of mechanical systems with frictional contacts.

These models in their primary form concern the case of a fully developed sliding on the contact area and possess singularity for the case of lack of the relative motion. The applied regularization occurred to be an effective method to avoid that problem and take into account different values of static and kinetic friction coefficients. The drawbacks are the stiff differential equations and the change of physical properties of the system near the stick mode.

In order to test the developed models of friction forces, a mathematical model of a special mechanical system is built, which is some modification of the disk-on-a-disk system analyzed in the works [7, 8], being a strongly simplified disk clutch. It is expected that the proposed model can exhibit much richer bifurcational dynamics, allowing for testing different aspects of friction models. It should be noted that the presented work is in progress and only preliminary results are reported. It is also considered the construction of the corresponding experimental rig in the future.

Acknowledgments

This work has been supported by the Polish National Science Centre, MAESTRO 2, No. 2012/04/A/ST8/00738.

References

- [1] Contensou, P. Couplage entre frottement de glissement et de pivotement dans la théorie de la toupe. In: Ziegler H. (Ed.), *Kreiselprobleme Gyrodynamik, IUTAM Symposium Celerina*, Springer-Verlag, Berlin, 1962, 201-216.
- [2] Zhuravlev, V.P. The model of dry friction in the problem of the rolling of rigid bodies. *Journal of Applied Mathematics and Mechanics* 6, 5 (1998), 705-710.
- [3] Kudra, G., Awrejcewicz, J. Approximate modelling of resulting dry friction forces and rolling resistance for elliptic contact shape. *European Journal of Mechanics A/Solids* 42 (2013), 358-375.

- [4] Kudra G., Awrejcewicz J. Regularized model of coupled friction force and torque for circularly-symmetric contact pressure distribution. *Proceedings of the 11th Conference on Dynamical Systems - Theory and Applications*, Lodz, 2011, 353-358.
- [5] Kudra, G., Awrejcewicz, J. A smooth model of the resultant friction force on a plane contact area. *Journal of Theoretical and Applied Mechanics* (2015), to appear.
- [6] Stamm, W., Fidin, A. Regularization of 2D frictional contacts for rigid body dynamics, *IUTAM Symposium on Multiscale Problems in Multibody System Contacts*, Springer, Dordrecht, 2007, 291–300.
- [7] Stamm, W., Fidin, A. Radial dynamics of rigid friction disks with alternating sticking and sliding. *Proceedings of the 6th EUROMECH Nonlinear Dynamics Conference*, Sankt Petersburg, 2008.
- [8] Fidin, A. Stamm, W. On the radial dynamics of friction disks. *European Journal of Mechanics A/Solids* 28, 3 (2009), 526-534.

Grzegorz Kudra, Ph.D., D.Sc.: Lodz University of Technology, Department of Automation, Biomechanics and Mechatronics, Stefanowski St. 1/15, 90-924 Lodz, Poland (grzegorz.kudra@p.lodz.pl). The author gave a presentation of this paper during one of the conference sessions.

Jan Awrejcewicz, Professor: Lodz University of Technology, Department of Automation, Biomechanics and Mechatronics, Stefanowski St. 1/15, 90-924 Lodz, Poland (jan.awrejcewicz@p.lodz.pl).